Turkish Journal of Electromechanics and Energy
ISSN: 2547-975X
Vol:8, No:2, Page 43-55 (2023)
https://www.scienceliterature.com

The effect of material change on system performance in compact plate heat exchanger design

K. Cebeci[1], S. Güçlüer[2, *]

[1]*Research & Development Department, Bosch Corporation, Manisa, Türkiye*

[2]*Department of Mechanical Engineering, Aydın Adnan Menderes University, Aydın, Türkiye*

ARTICLE INFO

***Article Type*:**
Research Paper

Article History:
Received: 10 July 2023
Revised: 28 August 2023
Accepted: 3 September 2023
Published: 15 October 2023

Editor of the Article:
M. E. Şahin

Keywords:
Heat exchanger
Combi boiler
AISI 304L, 316L
Burst resistance

ABSTRACT

As a component of residential comfort systems, compact plate heat exchangers facilitate access to domestic heated water. Due to the increased demand for these solutions on the market, it has become more challenging to acquire the necessary production materials. To overcome this challenge, it is essential to implement intelligent, cost-effective solutions. This study aimed to examine and compare the influence of using different materials (AISI 304L and AISI 316L), for the top layer plate of compact brazed plate heat exchangers, on the operational efficiency of the component. The thermal performance and burst resistance of products are considered in performance evaluations. The outcome of the experimental procedure was evaluated using the methodology of finite element analysis. The Finite Element Analysis (FEA) platform was established to validate the outcomes of pressurization experiments. This innovative technology streamlines the evaluation of pressurization tests by allowing us to confirm field data without incurring additional expenses. Furthermore, this study leverages this FEA simulation platform to explore the feasibility of alternative materials for the intended applications.

Cite this article: K. Cebeci, S. Güçlüer, "The effect of material change on system performance in compact plate heat exchanger design," *Turkish Journal of Electromechanics & Energy*, 8(2), pp.43-55, 2023.

1. INTRODUCTION

In recent years, the developments in clean, renewable, and efficient energy policies have enabled to design of new and innovative heat exchangers [1]. Heat exchange devices are essential components in complex engineering systems related to energy generation and energy transformation in industrial scenarios. There is more than one method developed for heat exchanger design analysis. For example, Fernandez-Seara *et al.* provided an overview of the Wilson plot approach, as well as several changes offered by researchers over the years to increase its accuracy and broaden its application to a wide range of convective heat transfer problems. This information will undoubtedly be valuable to thermal design engineers [2]. The design and operation principles of plate heat exchangers (PHEs) are well described in the works of Wang *et al.* [3], Shah and Sekulic [4], and Tovazhnyansky *et al.* [5].

Akdari *et al.* showed that crystal plasticity and finite element analysis in metal forming may accurately predict thickness distribution. The multiscale modeling technique provides a foundation for developing innovative PHEs with improved thermomechanical characteristics and lower production costs [6]. Gürler conducted a study on plate heat exchangers with different chevron angles at inner channels, using tensile testing and finite element analysis (FEA) as the primary methodologies [7]. Hayta investigated plate heat exchanger metal fatigue in different materials. Fatigue testing was carried out on copper-brazed 316L and 304L stainless steel PHEs. The mechanical properties of brazed and non-brazed steel specimens were investigated by tensile testing and microstructural analysis [8]. A numerical simulation was performed on a local element-by-element basis using the Effectiveness-Number of transferred units (e-NTU) method to simulate the heat exchanger by Manigandan *et al.* The heat exchanger's chevron angle determines the friction factor, which is used to calculate the Nusselt number. The experiment uses different plates, fluid flow rates, and intake and output temperatures [9].

The use of low-silver-content filler metals is considered economically advantageous. Fukikoshi *et al.* presented a study aimed to investigate the brazing capability of a brazing filler metal with a low silver content when applied to copper and SUS304. A satisfactory joint was achieved, and a significant dissolution reaction took place at the copper interface [10]. Gatea *et al.* studied incremental sheet formation and process factors. Flexible forming using incremental sheet forming (ISF) is new. The method is cost-effective and easily automated for various applications since it adapts to ordinary milling machines and

*Corresponding author's e-mail: sgucluer@adu.edu.tr

requires little equipment, dies, and forming presses. This study provides a thorough review of the current state of ISF techniques, including their technological capabilities and restrictions, as well as their process parameters and their effects [11].

Way *et al.* provided valuable information regarding brazing and its long-standing use as a joining procedure. Brazing has attracted attention recently because it can help create future technologies including fusion energy, solid oxide fuel cells, and nanoelectronics. Brazing has also helped advance automobile light weighting by solving aluminum-to-steel connecting issues. The introduction of filler metals has enabled various applications. This overview covers brazing theory and practice with a focus on filler metals. It also discusses advanced filler metal research and prospects [12].

Erdemir *et al.* investigated the possibility of using AISI 304L instead of AISI 316L for plate heat exchangers while preserving operating efficiency and performance. The present research examined the corrosion of AISI 316L and AISI 304L stainless steel under simulated service circumstances. AISI 304L, which is more cost-effective, was tested to replace AISI 316L. Plate heat exchangers were tested for temperature, pH, and solution chloride ion concentration. Electrochemical corrosion tests evaluated the pitting properties of the two stainless steel materials under simulated operation settings and pitting corrosion-specific test parameters [13].

A failure analysis of stress corrosion fracture in heat exchanger tubes during start-up operation has been performed by Xu *et al.* on shell tube heat exchangers, which are not directly related to compact plate heat exchangers. This situation is comparable to that of C-PHEs, and similar crack detection methods have been investigated [14]. Hussaini *et al.* conducted a study and the formability of AISI 316 at high temperatures is being investigated experimentally and numerically. The objective of this study is to examine the formability of austenitic stainless steel 316 under elevated temperatures. The formability of deep drawing can be evaluated based on the limiting drawing ratio and the thickness of the drawn cup [15].

Jayahari *et al.* used LS-DYNA to investigate austenitic stainless steel 304 formability and aluminum (Al) friction factor in deep drawing setups at increased temperatures. The current investigation deep draws austenitic stainless steel (ASS)-304 with different blank diameters under heated circumstances. The drawn cups showed a significant increase in the limitation of drawing ratio (LDR) from 2.16 at ambient temperature to 2.5 at 150 °C [16]. The numerical analysis of the BPHE channel plate section by Bjorn Persson provides a method and steps. This study investigates the reduction in material thickness and formability of sheet metal geometry. Examining finite element analysis and physical testing. By comparing finite element analysis and physical experiments, the results were confirmed [17].

To enhance the performance and miniaturization of the absorption system, it is necessary to accurately predict the performance of a plate heat exchanger used as a solution heat exchanger. Ham *et al.* investigated the thermal performance of solution heat exchangers under operating conditions of the solution heat exchanger in the double-effect absorption system, and new correlations of the Nusselt (Nu) number and Fanning friction factor were devised and compared [18]. Li *et al.* designed a thermal performance model of the brazed PHEs developed with flow maldistribution among channels taken into account. Using the experimental results, the proposed model is validated [19]. Will *et al.* explained a method regarding the estimation of the local heat transfer coefficient of the primary fluid (refrigerant) and its distribution to the channels [20].

To reduce the cost of plate heat exchangers in combi boilers, the availability of AISI 304L and AISI 316L materials, specifically in a thickness of 0.5 mm rather than 1 mm was confirmed by the material suppliers. During negotiations, it was disclosed that sheets with thicknesses of 0.3 mm, 0.5 mm, and 1 mm were viable options for use in the relevant materials. It was determined that the interior plate's thickness of 0.3 mm would not be optimal for the outer plate. This argument is based on the idea that the upper plate is the primary barrier against external impacts. It is claimed that a thickness of 0.3 mm is insufficient to effectively fulfil this protective function. In addition, it is noted that plates with a thickness of 0.3 mm can experience post-processing contraction, also known as "undulation." which can lead to visually deformed products. As an alternative to the currently used 1 mm thickness of 316L, 0.5 mm thick plates of 304L and 316L were selected as the material for the upper plate. In addition, a series of tests has been devised to evaluate the parameters associated with this modification. This study investigates the application of mechanical strength tests and thermal function tests to analyze the effects of material variations in the top plate of 0.5 mm-thick 304L and 316L. Following the completion of the experiments, the acquired data was subjected to analysis.

2. EXPERIMENTAL

2.1. Functional (Thermal Performance) Test

Compact plate heat exchangers (C-PHEs) with a plate count of 26 were used in the experiments. Three different samples were tested. Plate heat exchangers are produced with 0.5 mm top plates in 304L and 316L. The heat exchangers were then subjected to the first functional test. The minimum and maximum ranges of heat output and domestic hot water (DHW) temperature requirements for each plate number were the acceptance criteria for this test. The findings were positive, and the associated output values were evaluated.

The test description is as follows: Establish a connection between the plate heat exchanger (PHE) system and the designated test platform. Initiate the process by opening the valve, activating the combi system, and thereafter concluding the Thermal Performance Monitoring (TPM) procedure. In addition, it is advisable to open the bypass and central heating lines. An increase in pressure is required. The pressure is within the range of 2.5 to 2.8 bar. The circulation of water via the central heating (CH) line should continue until the temperature reaches 71.5°C. To finalize the CH circuit, it is necessary to close the valves and activate the pump. Minimize the temperature of the housing of the plate heat exchanger. To remove hot water, it is necessary to release drain valves. During the heating process, it is necessary to remove PHEs. Upon completion of data collection, the experiment was concluded.

2.1.1. Operational Parameters and Experimental Configuration

There are six Equipment Under Test (EUTs) in total, each comprising top and bottom plates made of 304L and 316L stainless steel. The thickness of these plates is 0.5 mm.

- The medium being addressed is water.
- The initial temperature of the CH is 72˚C.
- The recorded outlet temperature of the CH is 51˚C.
- The initial temperature of the Direct Cold Water (DCW) is 10˚C.
- The recorded DHW temperature is 60˚C.
- The pressure of the CH system is 1.5 bar.
- The domestic hot water (DHW) system operates at a pressure of 10 bar.

The measurement point involves evaluating the system's heat output by calculating the ratio of inlet and outlet temperatures and then comparing it to the optimal range.

The steps for calculating C-PHE performance were briefly presented by Gullapalli [21]. The following equation is used to calculate heat output, effectiveness, and heat capacity.

$$Q_{DHW} = m_{DHW} C_p \Delta T \quad (1)$$

$$\mathcal{E}_{DHW} = \frac{Q_{DHW}}{Q_{max}} \quad (2)$$

$$\mathcal{E}_{CH} = \frac{Q_{CH}}{Q_{max}} \quad (3)$$

$$Q_{max} = C_{min}(T_{Ch,in} - T_{DCW}) \quad (4)$$

$$C_{min} = C_{DHW} = m_{DHW} c_p,\ m_{DHW} < m_{CH} \quad (5)$$

Equation (1) calculates domestic hot water (DHW) heat transfer, where Q_{DHW} is heat transfer, m_{DHW} is water mass, and C_p is specific heat capacity in kilojoules per kilogram per degree Celsius. Equation (3) calculates the efficiency of the PHE in the CH line ($\mathcal{E}_{CH}$). The maximum potential heat transfer rate (Q_{max}) in kilowatts (kW) can be calculated by multiplying the minimum heat capacity rate (C_{min}) by the temperature difference between the hot fluid inlet temperature at the CH line and domestic cold-water temperature. C_{min}, the heat capacity of domestic hot water (DHW), equals C_{DHW}. Heat capacity, C, is the amount of heat energy needed to raise a substance's temperature by one degree Celsius. Since the domestic water flow rate is lower than the central heating water flow rate, multiplying the domestic water mass flow rate by specific heat capacity yields this result.

C. Büyükaşık made extensive calculations in his study and suggested that the newly developed plate heat exchangers involve the use of curved channels as opposed to straight channels exhibit superior efficiency compared to some geometries documented in the current literature [22].

2.1.2. Functional Test Equipment

Test equipment includes a combi-heated tank as shown schematically in Figure 1. The actual picture of the test setup is also shown in Figure 2. Water flowing through this tank heats the primary plate heat exchanger in a closed-loop system. The heated heat exchanger controls the CH line water temperature and determines the plate heat exchanger under test CH inlet temperature. Both sides of the test sample have temperature sensors. These devices record exit point temperatures once fluid temperatures entering the product reach the appropriate value. These recorded values are used to calculate performance characteristics.

Chevron angle modification and nano liquid between plates can improve heat exchanger heat transfer. G. Peker examined how geometries, flow rates, and concentration ratios affect used values. The total heat transfer rate and plate heat exchanger effectiveness increase with turbulent density [23]. Mehrarad et al. investigated the use of nanoparticles in common fluids in plate heat exchangers to increase thermal performance [24].

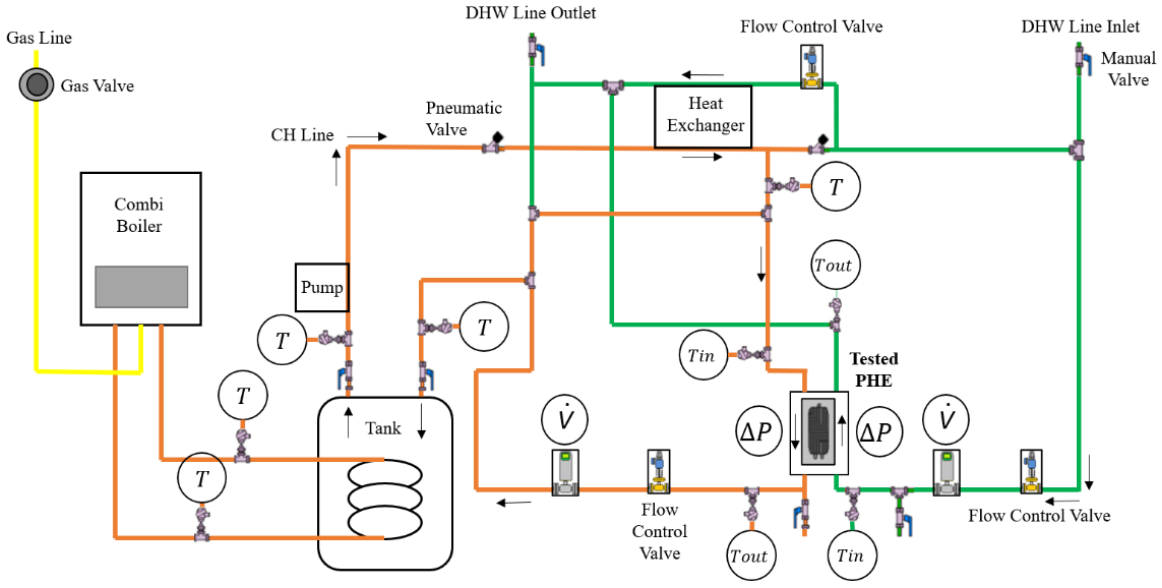

Fig. 1. The functional test equipment that was used in this study is shown schematically.

A similar experimental comparison of energy consumption and heat transfer performance of corrugated H-type and L-type brazed plate heat exchangers was conducted by Gungor [25]. Also, heat exchanger performance is significantly reduced in the presence of impurities in one or both fluid streams, frequently by deposits of inversely soluble salt [26].

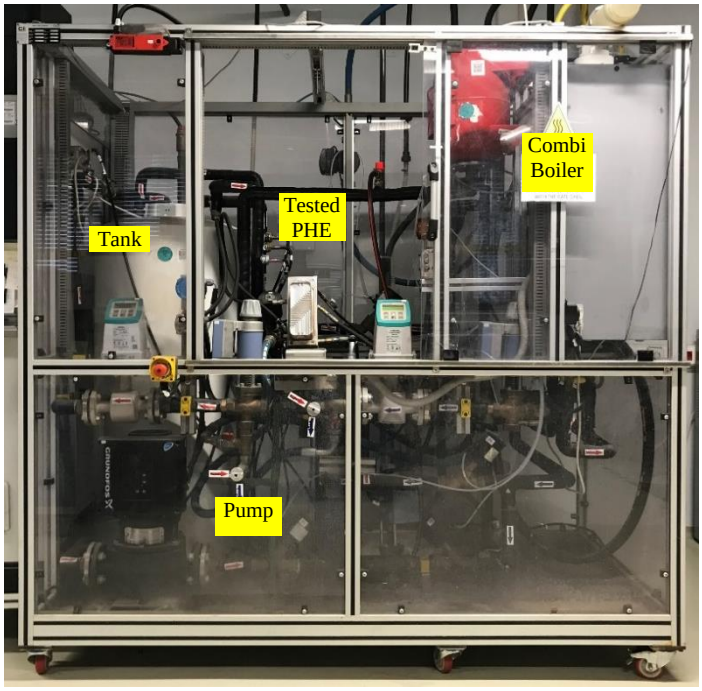

Fig. 2. Functional test kit. Test equipment includes a combi-heated tank. Water flowing through this tank heats the primary plate heat exchanger in a closed-loop system.

2.2. Mechanical Strength Performance (Burst) Test

Burst performance tests have been applied at 36 bar to observe the top plate material deformation and internal leakage status by exceeding the recommended test pressure value of 15bar which is the maximum working pressure (10 bar) times factor of safety value (1.5) defined in section 6.2.1.1. of BS EN 625:1996 Gas-fired central heating boilers – Specific requirements for the domestic hot combination boilers of nominal heat input not exceeding 70 kW.

Burst tests are being utilized to assess the static loads generated by domestic pressure and the designated application time for various purposes such as:

- Identification of the maximum burst pressure,
- Design margin confirmation of the production part,
- The factor of safety evaluation,
- Failure mode determination (how a part fails),
- Finding the ‘weakest link’ in a production or assembly.

2.2.1. Method and Experimental Configuration

The quantity of EUTs (Equipment Under Test) is 5, consisting of top and bottom plates made of 304L and 316L stainless steel with a thickness of 0.5 mm. The test specimen is attached to the experimental apparatus. The samples to be tested are placed on the appropriate block, which is selected based on the number of plates, and then connected to the apparatus.

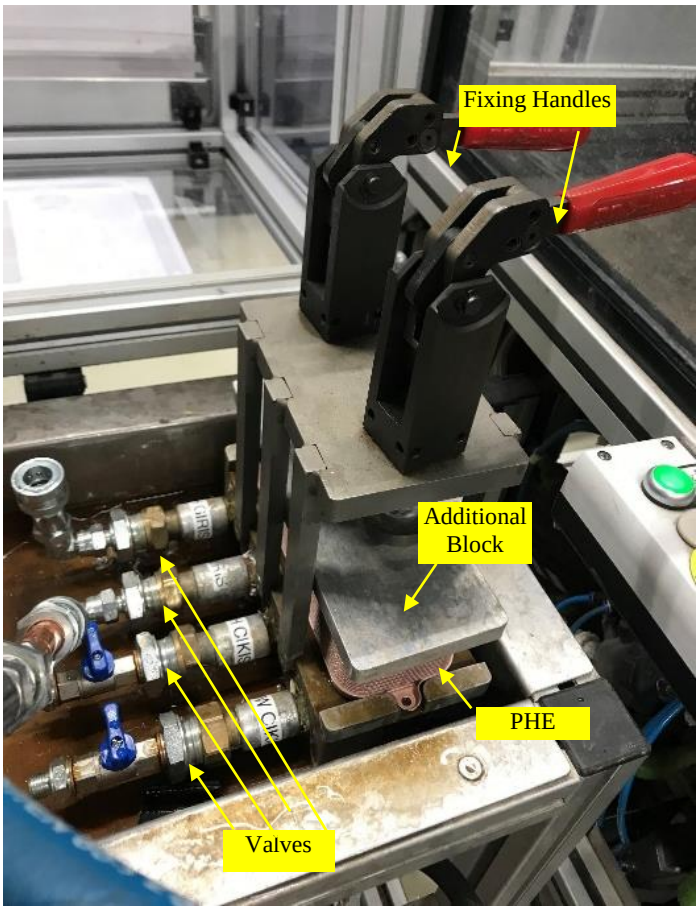

Fig. 3. PHE holding stand.

The specimens to be investigated are mounted to the indicated sites, as shown in Figure 3, with the apertures orientated downwards, using the testing platform's supporting mechanism. Burst test apparatus inlet details are given in Figure 4. The load profile of the applied burst test is shown in Table 1.

In the PHE, valves 1 and 4 pressurize CH lines, which is not needed for home line pressure testing. To raise the pressure in valve 2's domestic line pipe. The valve must be opened during test initiation. The first opening of valve 3 prevents air from trapping in the sample. The valve is closed while the water is moving after confirming the absence of air in the previous sample. The valve 4, which detects test sample leakage, should always be open. The CH line and Domestic line are independent PHE system fluids that must not be mixed. At high pressures, the brazing points that link the CH and DCW lines may be damaged. This impairs component functionality owing to pressure loss. Following that, the test instrument is securely sealed with an impermeable mica glass cover intended to withstand water pressure. The technique that follows entails setting the device to the desired pressure level.

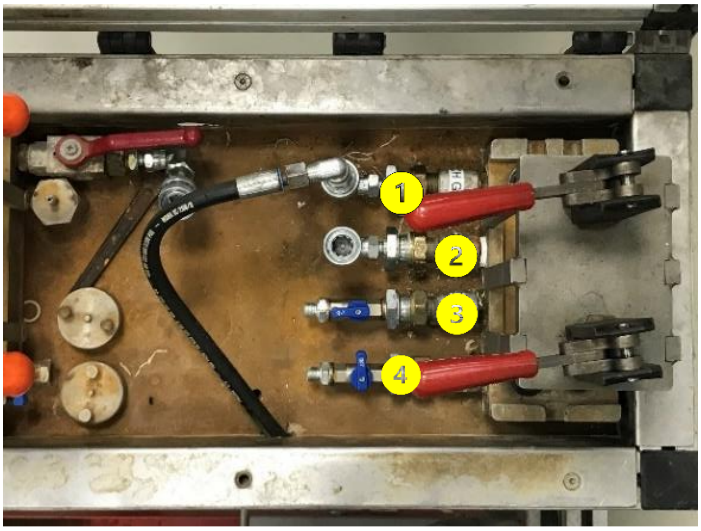

Fig. 4. Burst test apparatus inlet details.

In the PHE, valves 1 and 4 pressurize CH lines, which is not needed for home line pressure testing. To raise the pressure in valve 2's domestic line pipe. The valve must be opened during test initiation. The first opening of valve 3 prevents air from trapping in the sample. The valve is closed while the water is moving after confirming the absence of air in the previous sample. The valve 4, which detects test sample leakage, should always be open. The CH line and Domestic line are independent PHE system fluids that must not be mixed. At high pressures, the brazing points that link the CH and DCW lines may be damaged. This impairs component functionality owing to pressure loss. Following that, the test instrument is securely sealed with an impermeable mica glass cover intended to withstand water pressure. The technique that follows entails setting the device to the desired pressure level.

At the specified pressures, water is discharged from the Maximator and reaches the EUT. Burst test apparatus pressurizer (Maximator) is shown in Figure 5. Maximator is a pressurizer with an air filter regulator coupled to a high-pressure pump that may also be used manually. The digital manometer can be used to directly measure pressure within the system

The pressurization valves are progressively loosened in the absence of any water leaks. Afterwards, the initially closed valves 1 and 3 are partially opened to discharge the water from the heat exchanger that has been subjected to pressure. The C-PHE component is removed from the experimental apparatus and visually examined for any indications of swelling or deformation in the upper and lower regions of the heat exchanger. The top plates of the deformed samples were measured with the probe using the specified locations shown in Figure 6 as references.

The centre measuring point is independent of the domestic pressure field. Thus, the point was used as the reference point in the final samples, and deviations were calculated by comparing it to the other points. Figure 7 shows the upper plate projection of the surface via which the main pressure is directly delivered into the system.

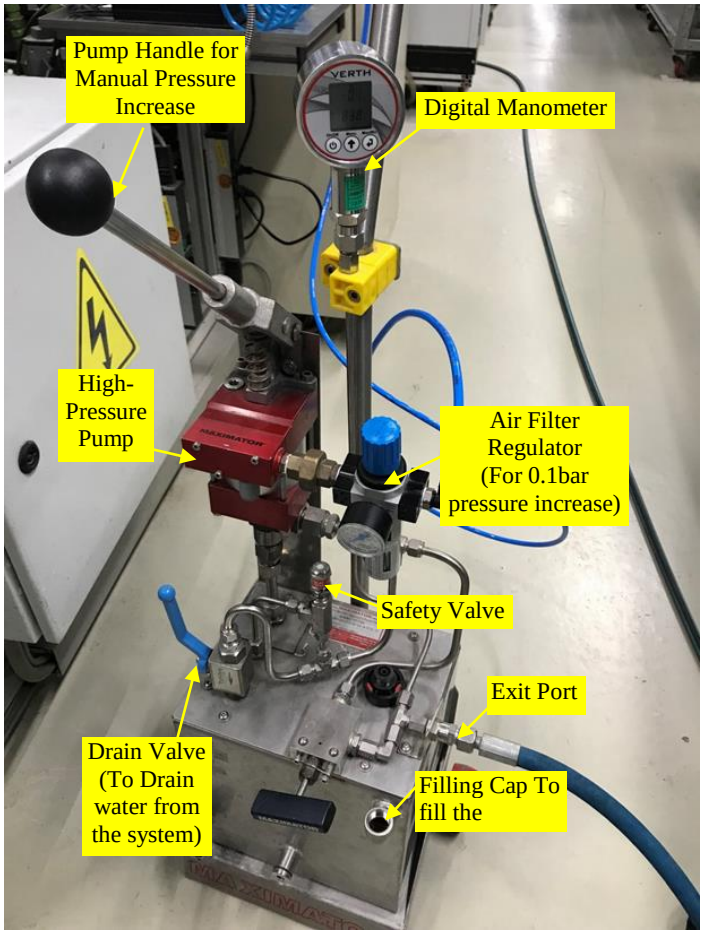

Fig. 5. Burst test apparatus pressurizer (Maximator).

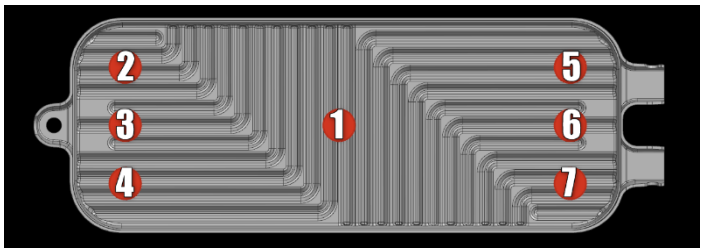

Fig. 6. Reference points for probe measurement.

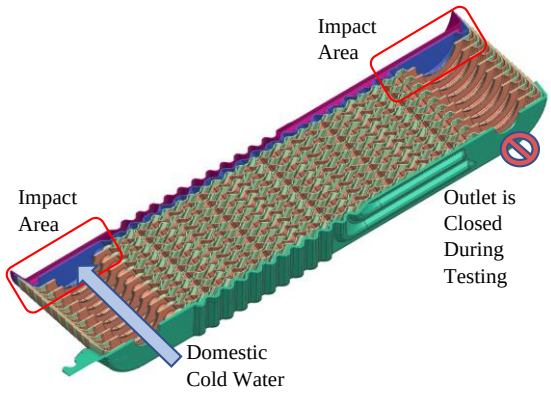

Fig. 7. Demonstration of impact area.

The fourth surface is the upper plate projection from which heated mains water exits the plate heat exchanger. For evaluation reasons, the results of measurements gathered at these points are the most essential. These surfaces are in vertical contact with the water flow and interact directly with the high mains pressure. The result of the force effect of the relevant pressure on the unit surface area multiplied by the pressure value at the vertical contact point is interpreted.

The probe measuring device shown in Figure 8 is a tool that allows measuring distances by taking point measurements at different reference points after a specified reference. The probe head and the planar elements it contains are very useful for the metric measurement of uneven surfaces, which are also found on the top plate of the plate heat exchanger. The amount of deformation that occurred in the plate heat exchanger sample produced with 316L/304L 0.5 mm top plate by this method was measured.

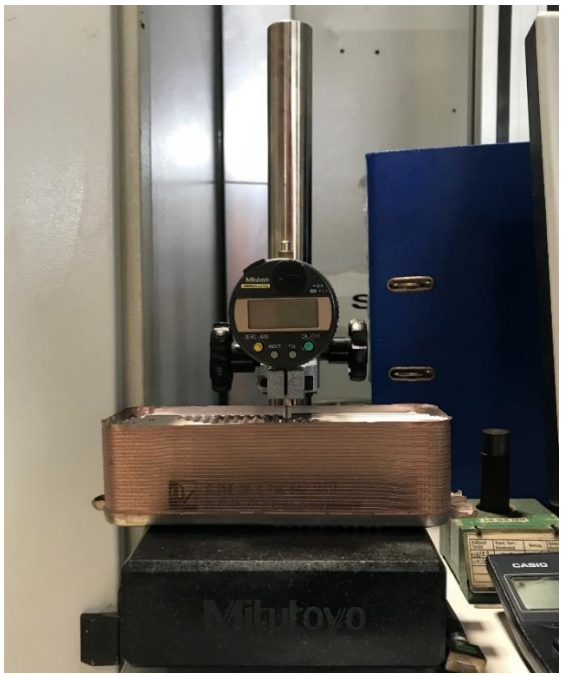

Fig. 8. Probe measurement device.

During the testing procedure, a probe measuring device was used to quantify the degree of deformation, an electronic pressurization element was used to apply pressure, and fixing element materials were used to maintain the heat exchanger in a constant state. The prescribed technique outlined in Table 1 was used to pressurize the test components, and the deformation quantities at the designated locations depicted in Figure 7 were recorded at six-bar intervals. Thus, a significant correlation was established between the applied load and the upper plate's deformation. To improve the dependability of the test results, an alternative measurement method was used. After applying sufficient pressure (particularly, 36 bar) to the material and obtaining the necessary level of deformation. The various EUTs were examined by cross-sections applied to the deformation surfaces, as shown in Figure 9. Deformed channel dimensions have been measured by the scaling method with the usage of Image-J.

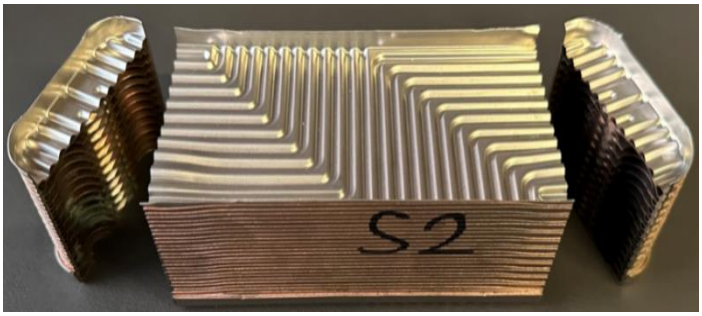

Fig. 9. 36 bar Used (DCW line) PHE sample cut-out image.

Table 1. Load profile of applied burst test.

Applied pressure (bar)	*Time under pressure (min)*	*Checkpoint*
16	3	The pressure loss of the manometer clock pointer and the water discharge of the heat exchanger are visually examined. This valve 4, which detects test sample leakage, must remain open at all times. Water is caused by leaks.
12	3	
18	3	
24	3	
30	3	
36	3	

2.3. FEA for Burst Test Result Validation (0.5 mm 316L Top Plate)

Experimental data was validated using FEA analysis based on controlled conditions and specified conclusions. A correlation was found when the analysis showed values similar to the experimental approach. Normal stress-induced surface deformation was evaluated using the ANSYS Transient Structural Module. The dynamic response of a structure under non-uniform and time-dependent loads can be assessed using this method. Flexible dynamic analysis is flexible for determining a structure's transient load-induced displacements, strains, stresses, and forces. Permanent connections are brazed regions in the numerical model. Because of this, numerical models were used to describe brazed zones in plate heat exchanger (PHE) samples using bonded contact. The frictional contact definition with a friction coefficient of 0.195 applies to all contact areas excluding brazed ones.

Depending on the topic, choosing the right form of contact can be difficult. New ANSYS users sometimes struggle to distinguish between frictionless, rough, frictional, and no-separation contact types. Bonded contact is the most common arrangement for surfaces, solids, lines, faces, and edges. Sliding or separation between bonded contact faces or edges is prohibited. The region is tightly bound as shown in Figure 10. This mode of communication allows linear resolution since the contact size or surface area remains constant during force application.

If mathematical contact is made, gaps will be eliminated and initial intrusion will be ignored. The symmetric quarter model method reduces finite element analysis (FEA) runtime due to symmetry in loads and component effects. This method applies just to structure surfaces and requires no user input. The displacement of a face with a symmetry plane requirement is constrained in the normal direction but not in the tangential direction.

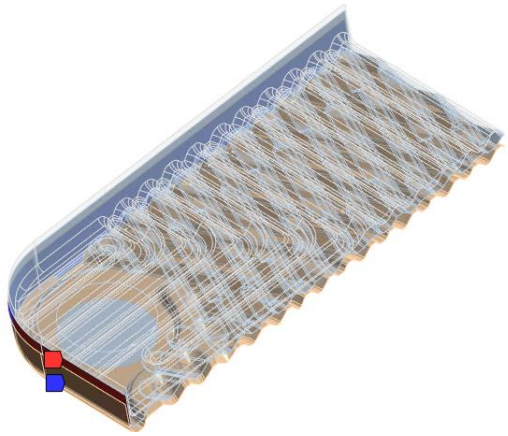

Fig. 10. C-PHE permanent contact surfaces.

2.3.1. Meshing

Meshing was accomplished using elements with an average size of 0.33 mm. A combination of 2D quadrilateral and triangular elements was used. The total number of nodes in use is 177,110. There are 171,081 elements in all. The illustration below shows the use of increasing element density in the building of blend corners.

2.3.2. Material Database

The Multilinear Isotropic Hardening material model was used to model the 316L steel. 316L Material properties are given in Table 2. The relevant material parameters were taken from the Ansys Granta Material database. The characterisation of material properties is an important first step in representing any material model using Finite Element Analysis (FEA). Incorrect inclusion of material details can have a significant impact on the outcome. Inaccuracies in the output of the Finite Element Analysis system are unavoidable due to the insertion of incorrect data. When introducing material parameters into Finite Element Analysis, it is critical to be cautious and attentive.

Table 2. 316L Material properties.

Property	*Value*	*Unit*
Density	7969.4	kgm^{-3}
Young's modulus	1.9736 x 10^5	MPa
Poisson's ratio	0.26995	
Bulk modulus	1.4298 x 10^{11}	Pa
Shear modulus	7.7703 x 10^{10}	Pa
Yield strength	229.57	MPa
Tangent modulus	1240	MPa
Isotropic thermal conductivity	14.886	$Wm^{-1}C^{-1}$
Specific heat constant pressure	509.61	$Jkg^{-1}C^{-1}$
Isotropic resistivity	7.476 x 10^7	Ohm.m

3. RESULTS

3.1. Functional (Thermal Performance) Test Results

Due to its varying component ratios, reducing the thickness of 304L, a distinct material family, requires numerous considerations. From these principles, formability, causality, and corrosion resistance matter most. To assess and understand new material effects, plate heat exchangers with 304L 0.5 mm top plates were functionally tested as shown in Table 3. As described in the methodology section, three unique samples of material with plate number of 26 were tested using a functionally specified testing apparatus. The elements' thermal conductivity function has been proven, and all samples have met the standards' output values.

Table 3. 304L Top plate used PHE functional test results.

		Acceptance Criteria			*Test Results*		
Description	*Unit*	*Nom*	*Min*	*Max*	*Sample 1*	*Sample 2*	*Sample 3*
CH flow rate	l/min	25.1	25	25.2	25.1	25.0	25.1
Temp. CH IN	°C	71.6	70.6	71.6	71.4	71.4	71.5
Temp. CH OUT	°C	51	49.5	52	50.8	50.8	50.8
DHW flow	l/min	10.1	10	10.2	10.1	10.2	10.1
Temp. DCW	°C	10	9	10	9.7	9.8	9.5
Temp. DHW	°C	60	59.5	61	59.5	59.7	59.6

Figure 11(a) Displays flow rate values and ranges between maximum and minimum allowed limits. For the 304L top plate used PHE CH flow rate is in the ideal status as expected since there is no change affecting internal flow dynamics such as a change in chevron angles of the internal plates. The flowmeter is being calibrated with an error rate of 1% of the displayed value. The flow rate of the system can be arranged with the pump modulation. Flow rate values can deviate until air is fully purged from the system. When the desired range is reached, the modulation stops, and the flow rate value remains constant. Figure 11(b) displays the temperature value of the plate heat exchanger central heating inlet for 304L top plate used PHE. To perform the necessary test system inlet temperatures must be arranged accordingly throughout the system. The error rate for CH inlet temperature reading is defined as ±1°C. The calibration process of the temperature sensor is being completed according to the mentioned range. Water temperature in the CH line is being increased by heat exchange between the water coming from the coil tank and CH line water.

Figure 11(c) displays the temperature value of the plate heat exchanger central heating outlet for the 304L top plate used PHE. This value is related to the efficiency of the component. Since the inlet point measurements are available, heat transfer with measured ΔT and Equation (4) can be calculated. The temperature value is being read by the temperature sensor. Figure 11(d) shows the flow rate values and the range between the maximum and minimum allowed limits. For the 304L top plate used PHE domestic cold water flow rate is in the ideal status as expected since there is no change affecting internal flow dynamics such as a change in chevron angles of the internal plates. Modulation of the domestic line is being arranged by valves placed within the system.

Figure 11(e) displays the temperature value of the plate heat exchanger domestic inlet line for 304L top plate used PHE also shown in Table 4. To perform the necessary test system inlet temperatures must be arranged accordingly throughout the system. The temperature value of the DCW inlet is arranged by the usage of the chiller. Figure 11(f) displays the temperature value of the plate heat exchanger domestic outlet line for the 304L top plate used PHE. This value is related to the efficiency of the component. Since the inlet point measurements are available, we can calculate the heat transfer with measured ΔT and Equation (4). After using the provided equations in section 2.1.1, the thermal performance parameters were calculated using the respective values for each sample. The performance parameters of the 0.5 mm 316L top plate utilized in the Plate Heat Exchanger (PHE) have been defined using a similar methodology and given in Table 5.

Table 4. Performance calculation results for 304L top plate used PHE (26 plates).

Description	*Unit*	*Average*	*Min*	*Max*	*Sample 1*	*Sample 2*	*Sample 3*
DHW heat output	kW	35.2	35.1	35.3	35.2	35.3	35.1
DHW effectiveness	-	0.308	0.306	0.311	0.308	0.311	0.306
CH heat output	kW	≥35	-	-	36.0	36.0	36.1
CH effectiveness	-	0.327	0.326	0.329	0.328	0.326	0.329

Table 5. 316L Top plate used PHE functional test results.

Description	*Unit*	*Nom*	*Min*	*Max*	*Sample 1*	*Sample 2*	*Sample 3*
CH flow rate	l/min	25.1	25	25.2	25.1	25.1	25.1
Temp. CH IN	°C	71.6	70.6	71.6	71.4	71.2	71.6
Temp. CH OUT	°C	51	49.5	52	51.0	50.4	51.0
DHW flow	l/min	10.1	10	10.2	10.1	10.2	10.1
Temp. DCW	°C	10	9	10	9.5	9.6	9.5
Temp. DHW	°C	60	59.5	61	59.5	59.6	59.6

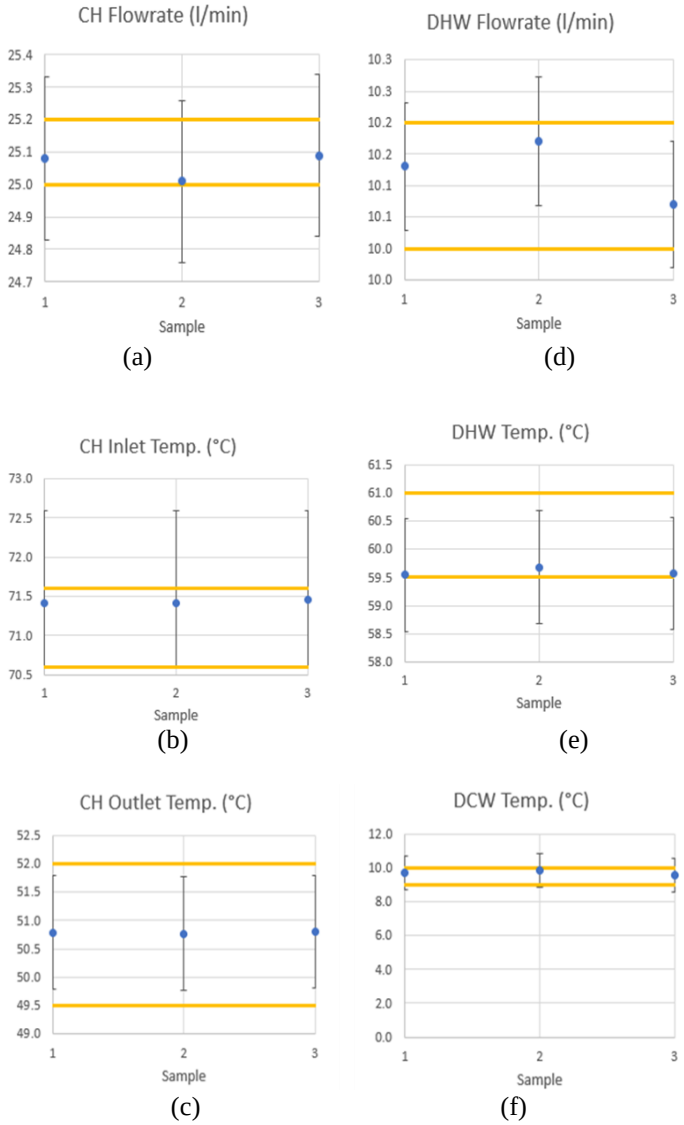

Fig. 11. 304L Top plate used PHE functional test results, (a) CH flow rate, (b) CH inlet temperature, (c) CH outlet temperature, (d) DHW flow rate, (e) DCW temperature, (f) DHW temperature.

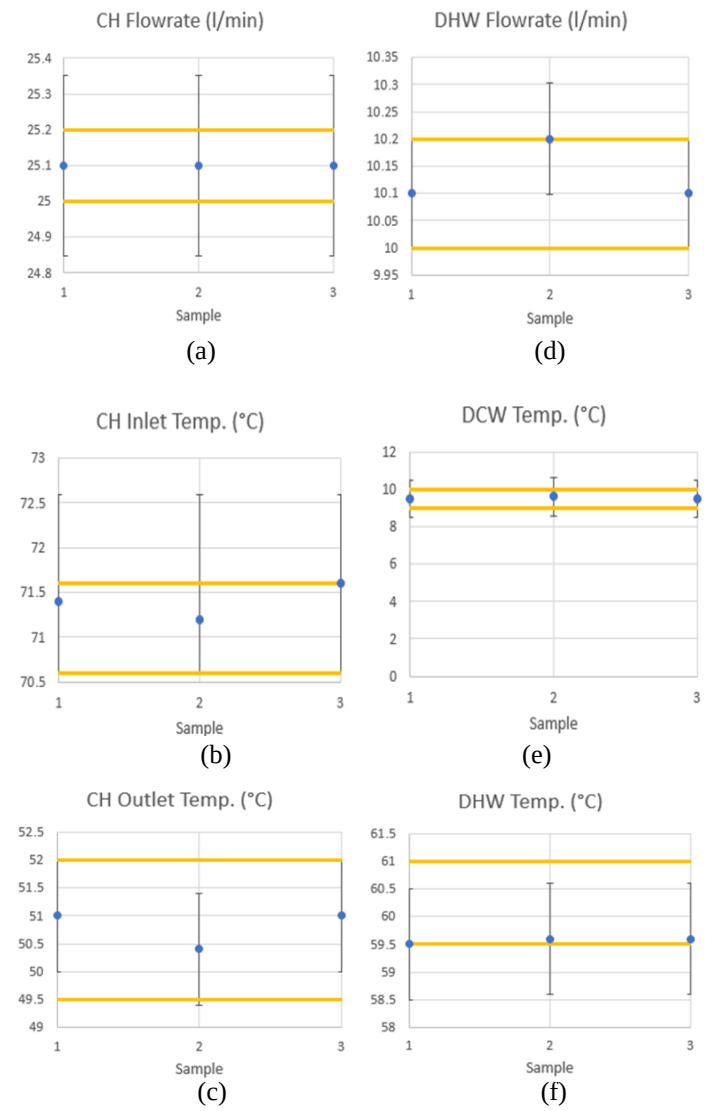

Fig. 12. 316L Top plate used PHE functional test results. (a) CH flow rate, (b) CH inlet temperature, (c) CH outlet temperature, (d) DHW flow rate, (e) DCW temperature, (f) DHW temperature.

Figure 12(a) displays the maximum and minimum flow rate values. PHE CH flow rate is optimal for the 316L top plate because there is no change in internal flow dynamics, such as internal plate chevron angles. The flowmeter's reported value is calibrated with a 1% margin of error. The modulation of a pump controls system flow. Until all air is expelled, the discharge rate can vary. When the target range is attained, the flow rate remains constant and modulation ceases. Figure 12(b) illustrates the temperature of the central heating inlet of a 316L top plate PHE plate heat exchanger. To conduct crucial testing, the system's inlet temperatures must be modified. The specified error rate for temperature readings at the CH inlet is 1°C. According to the range, temperature sensor calibration is performed. Heat transfer between the coil tank and the CH line water elevates the temperature of the CH line water.

Plate heat exchanger central heating outlet temperature for 316L top plate using PHE, as shown in Figure 12(c). This value indicates the efficacy of a component. Since inlet point data are known, heat transfer can be calculated using measured ΔT and Equation (4). Temperature value is received by the temperature sensor. Figure 12(d) depicts the flow rate values and the range between the maximum and minimum limitations. As anticipated, the PHE domestic cold water flow rate for the 316L top plate is ideal, as there is no change in internal flow dynamics, such as internal plate chevron angles. Modulating domestic lines are internal valves. Figure 12(e) depicts the domestic inlet line temperature of a plate heat exchanger with a 316L top plate using PHE. To conduct crucial testing, the system's inlet temperatures must be modified. The temperature of the DCW inlet is set by chiller equipment. Figure 12(f) displays the domestic outlet line temperature for 316L top plate PHE plate heat exchangers. This value indicates the efficacy of a component. Since inlet point data is available, heat transfer can be computed using measured ΔT and Equation (4). The thermal performance parameters were determined by applying the equations provided in section 2.1.2 to the corresponding values of each sample.

Table 6. Performance calculation results for 316L top plate used PHE (26 plates).

Description	*Unit*	*Average*	*Min*	*Max*	*Sample 1*	*Sample 2*	*Sample 3*
CH Heat Output	kW	36.0	35.7	36.3	35.7	36.3	36.0
DHW Heat Output	kW	35.3	35.3	35.4	35.3	35.4	35.3
CH Effectiveness	%	0.333	0.330	0.337	0.330	0.337	0.332
DHW Effectiveness	%	0.326	0.326	0.327	0.326	0.327	0.326

Connecting the relevant material to the test configuration, specifying the prescribed temperature levels at designated locations in the reference values, and then determining the temperature flow and pressure values of the fluid at the inlet and outlet points of the plate heat exchanger product were all part of the functional tests. Following the determination of these variables, the productivity of the sample was determined using relevant calculations and then compared to the acceptance requirements. Given the correlation between the material change in the upper plate and the water in the CH line, the significance of the CH line analysis results is of the uttermost importance to this investigation. The functional evaluations for plate heat exchangers with a 316L 0.5 mm top plate were performed on a set of 26 plates, and the findings were documented in Table 6.

The adjustment mentioned in this study is to the upper plate material, and it is expected that it will have little influence on thermal performance. However, because the reduction in material thickness (316L 0.5 mm Top Plate Usage) does not require a change in material composition, it does not affect the thermal performance characteristics.

This situation is unique to the 304L. The weld strength is expected to vary due to the material difference between the lower and higher plates, and it has been concluded that the thermal performance may be influenced accordingly. Using this information, a functional test was performed on plate heat exchangers with a 0.5 mm 304L top plate. The goal of the functional test is to read values from the device's screen such as adaptable pressure, temperature, and flow rate and use these numbers to compute the efficiency of the used heat exchanger product. The tests used three different amounts of samples from the 26 plate group. The results were positive, and it was demonstrated that the top plate material has no major effect on the functional performance of PHE because the main heat transmission occurs in the internal plates.

3.2. Burst (Mechanical Strength Performance) Test Results

A probe-measuring device is an instrument that is used to measure distances. This is accomplished by taking point measurements at various reference places following a predetermined reference. The probe head and its implemented planar parts are extremely useful in the context of metric measurement of non-uniform surfaces, such as those found on the upper plate of a plate heat exchanger. Table 7 contains the measurement and listing of the deformation that occurred in the plate heat exchanger sample, which was generated using a 316L/304L 0.5 mm top plate using the method stated in section 2.2.1.

Table 7. Top plate deformation corresponds to the applied pressure value.

Material	*Measurement point*	*At 6bar*	*At 12bar*	*At 18bar*	*At 24bar*	*At 30bar*	*At 36bar*
304L 0.5 mm top plate used PHE	1	0	0	0	0	0	0
	2	-0.67	-0.55	-0.44	-0.37	-0.25	-0.12
	3	0.09	0.11	0.12	0.15	0.37	0.45
	4	0.46	0.57	0.59	1.02	1.79	**2.54**
	5	0.10	0.12	0.13	0.13	0.15	0.28
	6	0.11	0.13	0.13	0.15	0.21	0.28
	7	0.12	0.25	0.53	0.97	1.47	**2.31**
316L 0.5 mm top plate used PHE	1	0	0	0	0	0	0
	2	0.28	0.28	0.29	0.29	0.35	0.42
	3	0.05	0.07	0.1	0.12	0.18	0.24
	4	0.28	0.29	0.29	0.31	0.72	**1.27**
	5	0.37	0.37	0.38	0.39	0.45	0.41
	6	0.25	0.27	0.29	0.32	0.39	0.43
	7	0.41	0.42	0.44	0.48	0.76	**1.07**

Throughout the experimental procedure, the specimen was subjected to pressure increases of 6 bars. At regular intervals, the ongoing process was suspended momentarily and a sample was extracted. The water within the sample was drained and the sample was transferred to the measuring device. The specimen was then transferred to the fixation platform and subjected to compression.

After reaching a pressure of 12 bar, the component was subjected to an isobaric procedure lasting 180 seconds. After the system was evacuated, successive deformation measurements were conducted and recorded on the heat exchanger. The procedure was carried out with exactness until a pressure of 36 bar was reached. The corresponding measurements were carefully recorded and then organized in a table. Five distinct samples were used and the mean values were calculated. Figure 9 depicts the deformed and subsequently cut plate heat exchanger sample, along with the corresponding surface designations.

In Table 8, overall channel dimension results are displayed. Deformation on the 12th channel is large since 304L material is more formable than the alternative. In Figure 13 304L Surface A values from Table 8 are displayed. With this graphic, channel height differences are easier to compare. This figure set covers 4 surfaces.

Table 8. 304L 0.5 mm Top plate used PHE cross-sectional deformation measurement results.

Channel number	*304L Surface A*	*304L Surface B*	*304L Surface C*	*304L Surface D*
	Channel Height (mm)			
1	3.312	3.282	3.411	3.284
2	3.362	3.388	3.305	3.284
3	3.319	3.261	3.263	3.305
4	3.323	3.261	3.312	3.263
5	3.305	3.282	3.305	3.298
6	3.337	3.303	3.305	3.326
7	3.284	3.24	3.305	3.284
8	3.326	3.303	3.39	3.284
9	3.337	3.324	3.347	3.326
10	3.358	3.303	3.305	3.326
11	3.358	3.346	3.39	3.326
The standard deviation of 11 channel	0.023	0.40	0.44	0.021
Average of 11 channel	3.329	3.299	3.330	3.30
12 deformed channel height	6.372	6.422	6.063	5.994
Measured max deformation (mm)	**3.042**	**3.122**	**2.732**	**2.693**

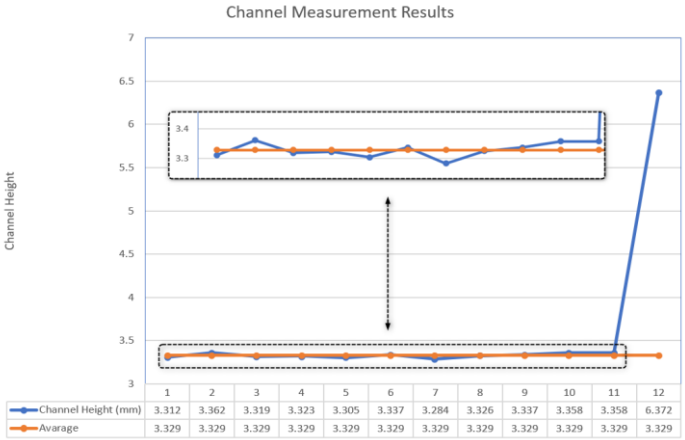

Fig. 13. Channel port dimension deviation for 0.5 mm AISI 304L top plate used PHE sample 1 surface A (36 bar Max).

In Figure 14 channel heights are quite similar and the standard deviation is calculated as 0.40. This value is different from surface A. The reason for that might be the spring back effect occurred after the cutting process. Smaller portion can lead to small differences and big portion is the opposite. For surface C similar comments are also validly made for surface D. There is no significant change between measured channel height values, but the 12th channel deformation is different. This is possible since force distribution on the top plate is not expected to be linear as calculated, displayed in Figure 15 and 16.

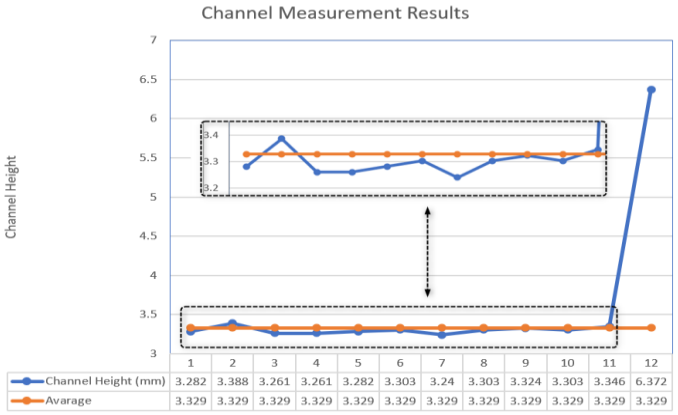

Fig. 14. Channel port dimension deviation for 0.5 mm AISI 304L top plate used PHE sample 1 surface B (36 bar Max).

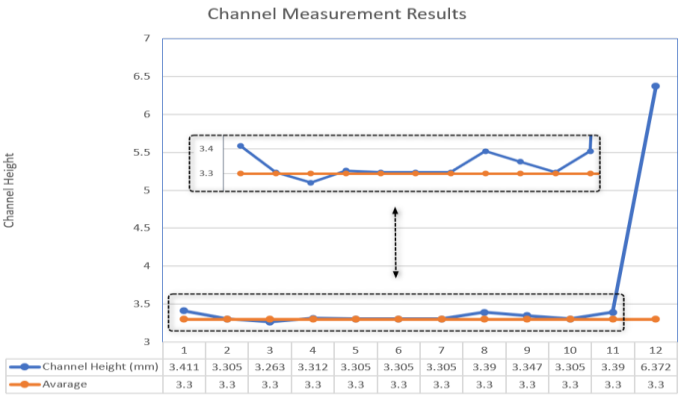

Fig. 15. Channel port dimension deviation for 0.5 mm AISI 304L top plate used PHE sample 1 surface C (36 bar Max).

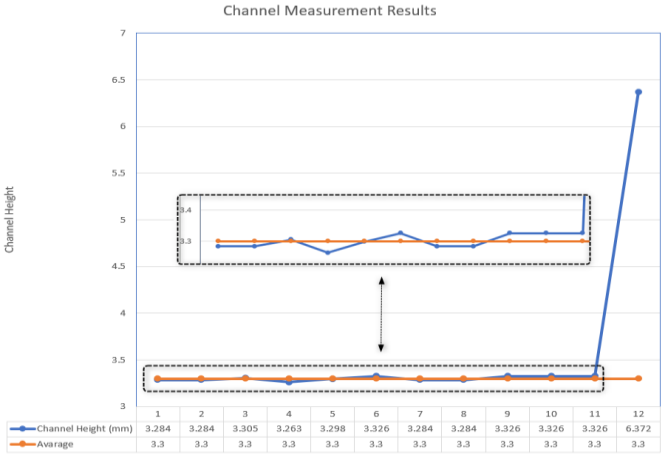

Fig. 16. Channel port dimension deviation for 0.5 mm AISI 304L top plate used PHE sample 1 surface D (36 bar Max).

The findings show that the heat exchanger constructed with a 316L top plate demonstrated reduced deformation compared to the plate heat exchanger utilizing 304L, despite both being exposed to identical loads and profiles as shown in Table 9. In the 9th channel, there is a significant reduction in channel height as shown in Figure 17(a). The reason for that might be the orientation error of the weight placed on the top of plates before the brazing process or simply an error that occurred from the vertical cutting process. Even with that decrease in channel height, no significant pressure loss occurred in the component. Surface B is near to mean body and values are similar as expected as shown in Figure 17(b). The last channel dimension is different due to the deformation on the endplate which is being transferred and became visible. Figure 17(c). displays the internal channel measurement results read from surface C which is shown in Figure 17(d).

Table 9. 316L 0.5 mm Top plate used PHE cross-sectional deformation measurement results.

Channel number	*316L Surface A*	*316L Surface B*	*316L Surface C*	*316L Surface D*
	Channel Height (mm)			
1	3.164	3.241	3.47	3.291
2	3.347	3.404	3.512	3.462
3	3.305	3.39	3.45	3.419
4	3.319	3.347	3.47	3.397
5	3.369	3.39	3.514	3.433
6	3.347	3.319	3.492	3.462
7	3.305	3.411	3.512	3.397
8	3.347	3.368	3.493	3.44
9	2.637	3.347	3.512	3.492
10	3.369	3.39	3.469	3.433
11	3.39	3.368	3.534	3.504
The standard deviation of 11 channel	0.20	0.04	0.02	0.05
Average of 11 channel	3.26	3.36	3.49	3.43
12 deformed channel height	4.26	4.11	4.58	4.48
Measured max deformation (mm)	**0.99**	**0.74**	**1.08**	**1.05**

Despite the initial specification in the CAD data for the inner plates of a 3.5 mm channel size, the data shown in Table 7. suggests a divergence from this value. It is related that during the fabrication step, a specified level of force is applied to the constituent and then maintained at that magnitude. The procedure is critical in promoting the formation of points of contact between the plates. Inadequate weight positioning to maintain duct size might result in compromised connection points, also known as brazing points, between the ducts.

The magnitude of 304L deformation was evaluated by performing cross-sectional cuts on the deformed samples and measuring the dimensions of the channels on four unique surfaces. The use of ImageJ has aided in the determination of values. In addition to these data, it was expected that spring-back phenomena could appear on the relevant surfaces, allowing them a degree of freedom following sectioning. The same procedure was utilized on a 316L 0.5 mm top plate with distorted PHE.

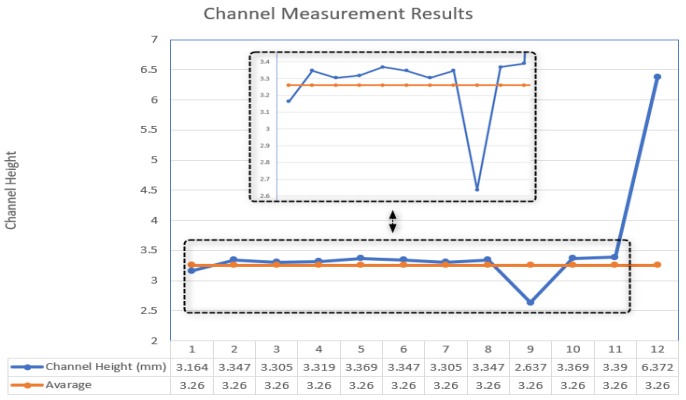

(a)

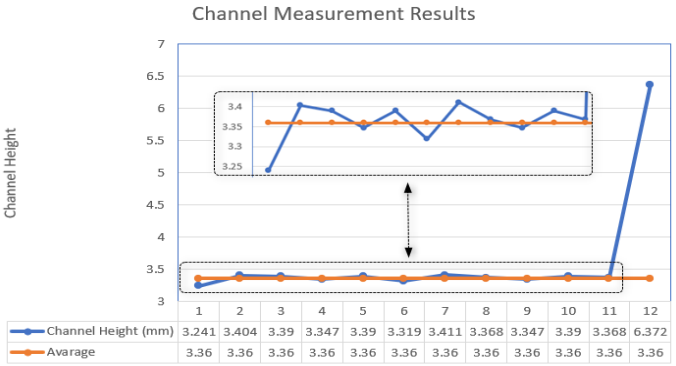

(b)

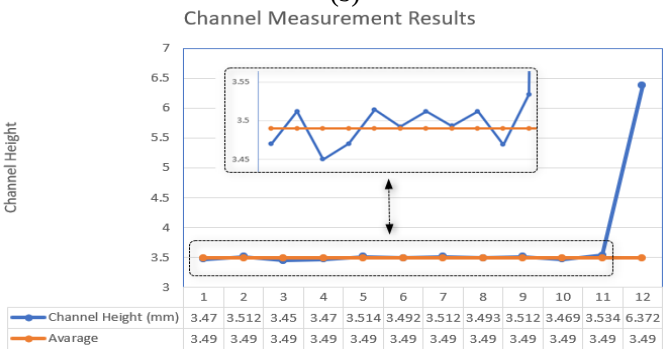

(c)

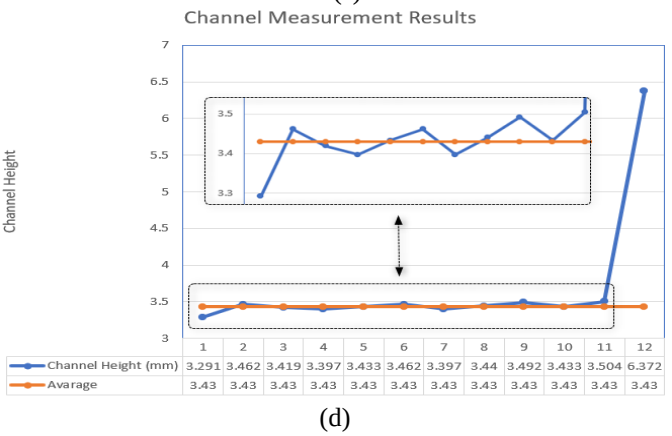

(d)

Fig. 17. Channel port dimension deviation measurement of the PHE sample manufactured with 0.5 mm AISI 316L top plate; Measurements were taken from (a) Surface A, (b) Surface B, (c) Surface C, (d) Surface D.

The internal channel measurements outlined in the previous section demonstrate a significant level of proximity to the measurement results observed in the sample of 304L used. Given that the internal plate materials and applied pressures are identical, it can be concluded that there is no substantial distinction among the internal channel heights.

3.3. FEA Results (Burst Test Result Confirmation of 0.5 mm 316L Top Plate Used PHE)

The data obtained from experimental methods was validated through the utilization of FEA. This analysis was conducted by considering controlled parameters and implementing established findings. The analysis demonstrated that there were values obtained in the experimental method that closely aligned with the results, and a correlation was established between them. Figure 18 presented below illustrates the stepwise representation of the time-dependent deformation value in finite element analysis.

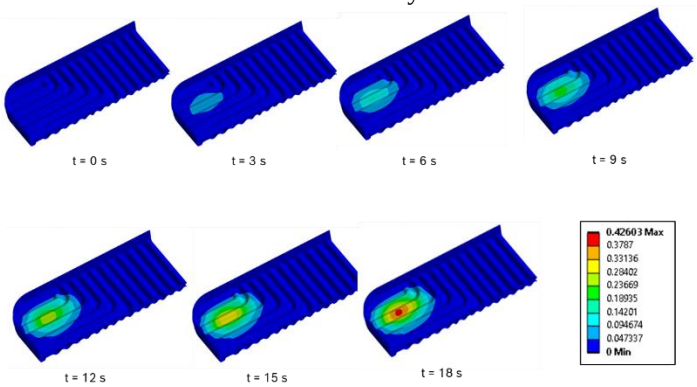

Fig. 18. Top plate deformation with timescale.

Based on the data presented in Figure 18, it can be observed that deformation initiates within the time interval ranging from 9k seconds to 12k seconds. The values under consideration are associated with a range of 20 to 25 bar.

The empirical evidence demonstrates that visible deformation takes place once the pressure reaches 24 bar, thus confirming the correlation between the experimental system and the finite element solution. A maximum deformation of 0.43 millimeters was observed following a gradual increase in 24 bar. The value obtained using the probe device is sufficiently like the relevant correlation to establish a relationship.

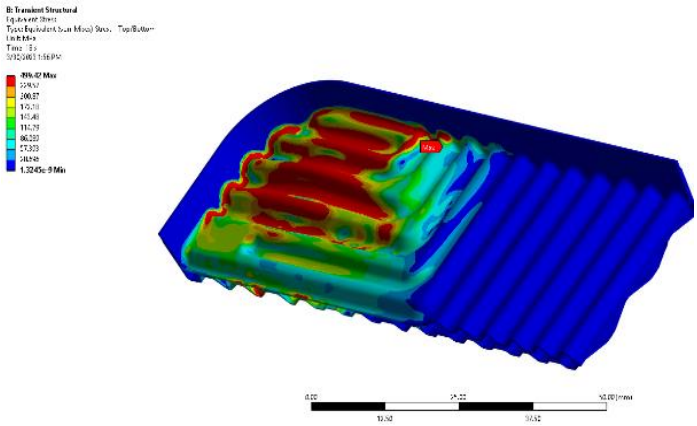

Fig. 19. Equivalent (Von-Misses) stress.

The material designated as 316L demonstrates a yield stress value of 229.57 MPa. The upper plate has been visually differentiated by the application of color coding, which serves to denote specific areas where stress values exceed the predetermined threshold limit. The regions are denoted by the color red. Figure 19 depicts the potential yield point that may occur on the component after the application of 36 bars of domestic pressure.

4. CONCLUSION

Plate heat exchangers with 304L and 316L 0.5 mm top plates were functionally tested. Tests showed favorable results. The products were then pressurized and tested for mechanical strength evaluation. When subjected to a pressure of 24 bar, the plate heat exchanger, which was built with a 316L top plate with a thickness of 0.5 mm, deformed. In contrast, the plate heat exchanger constructed with the same thickness of 0.5 mm 304L top plate displayed deformation at a lower pressure of 18 bar.

The study only looked at thermal performance and burst resistance; however, future research could broaden the scope to include lifespan performance, water hammer performance, and fouling resistance of the finished product.

In this study, a FEA platform was built to confirm pressurization experiment results. This technology simplifies pressurization test evaluation by verifying data in the field without cost. The study's FEA simulation platform is being utilized to examine alternative materials. Research is underway to find economically feasible materials that can improve high-quality product manufacture.

Acknowledgement

We thank Adem Özçelik and Erturan Yetişkin for fruitful discussions.

References

[1] M. Awais, and A. A. Bhuiyan, "Recent advancements in impedance of fouling resistance and particulate depositions in heat exchangers," *International Journal of Heat and Mass Transfer*, vol. 141, pp. 580-603, 2019.

[2] J. Fernandez-Seara, F.J. Uhia, J. Sieres, A. Campo, "A general review the Wilson plot method and its modifications to determine convection coefficients in heat exchange devices," *Applied Thermal Engineering*, vol. 27(17), pp.2745-2757, 2007.

[3] L. Wang, B. Sundén, and R. M. Manglik, *Plate heat exchangers: design, applications and performance*. Ashurst, Southampton: Wit Press. 2007.

[4] R. K. Shah, and D. P. Sekulic, *Fundamentals of heat exchanger design*. Hoboken, NJ: Wiley, 2003.

[5] L. L. Tovazshnyansky, P. O. Kapustenko, G. L. Khavin, and O. P. Arsenyeva. *PHEs in industry* Kharkiv, Ukraine: NTU KhPI, 2004.

[6] O. Onal, B. Bal, D. Canadinc, and E. Akdari, "Experimental and Numerical Evaluation of Thickness Reduction in Steel Plate Heat Exchangers," *Journal of Engineering Materials and Technology*, vol. 137(4), pp. 041008-041016, 2015.

[7] Y. Gürler, "Design and mechanical behaviour of brazed plate heat exchangers," Doctoral dissertation, Izmir Institute of Technology, İzmir Turkiye, 2018

[8] Y. Hayta, "Investigation of the Fatigue Behaviour of Metallic Components Used in Plate Heat Exchangers Under Variable

Dynamic Loads," Master's Thesis, Izmir Institute of Technology, Turkey, 2020.
[9] N. Manigandan, M, Suresh., V, NavenPrabhu. "Experimental Investigation of a Brazed Chevron Type Plate Heat Exchanger," *International Journal of Science Technology & Engineering*, 1(12), pp. 1-7, 2015
[10] T. Fukikoshi, Y. Watanabe, Y. Miyazawa, and F. Kanasaki, "Brazing of copper to stainless steel with a low-silver-content brazing filler metal," *In International Symposium on Interfacial Joining and Surface Technology (IJST2013), Osaka, Japan, November 27–29, 2013.*
[11] S. Gatea, H. Ou, & G. McCartney, Review on the influence of process parameters in incremental sheet forming. The International Journal of Advanced Manufacturing Technology, 87(1–4), pp. 479–499, 2016
[12] M. Way, J. Willingham, and R. Goodall, "Brazing filler metals," *International Materials Reviews*, 65(5), pp.257-285, 2020.
[13] H. Erdemir, "A study on stress corrosion cracking of plate-like heat exchangers and preparation of a test stand to investigate it," *Master Thesis,* Dokuz Eylül University, İzmir, Türkiye, 2017.
[14] S. Xu, C. Wang, and W. Wang, "Failure analysis of stress corrosion cracking in heat exchanger tubes during start-up operation," *Engineering Failure Analysis*, vol. 51, pp. 1-8, 2015.
[15] S. M. Hussaini, S. K. Singh, and A. K. Gupta, "Experimental and numerical investigation of formability for austenitic stainless steel 316 at elevated temperatures," *Journal of Materials Research and Technology*, 3(1), pp.17-24, 2014.
[16] L. Jayahari, P. V. Sasidhar, P. P. Reddy, B. B. Naik, A. K. Gupta, and S. K. Singh, "Formability studies of ASS 304 and evaluation of friction for Al in deep drawing setup at elevated temperatures using LS-DYNA," *Journal of King Saud University-Engineering Sciences*, 26(1), pp. 21-31, 2014.
[17] B. Persson, "Numerical analysis of a BPHE channel plate section," Master Thesis, Lund University, Lund, Sweden, 2011.
[18] J. Ham, J. Yong, O. Kwon, K. Bae, and H. Cho, "Experimental investigation on heat transfer and pressure drop of brazed plate heat exchanger using LiBr solution," *Applied Thermal Engineering*, vol. 225, pp. 120161, 2023.
[19] W. Li, and P. Hrnjak, "Effect of single-phase flow maldistribution on the thermal performance of brazed plate heat exchangers," *Applied Thermal Engineering*, vol. 219, p.119465, 2023.
[20] T. Will, L. Schnabel, and J. Köhler, "Detailed Thermal Evaluation of Brazed Plate Heat Exchanger Using Infrared Thermography," *Chemie Ingenieur Technik*, 95(5), pp. 732–739, 2023.
[21] V. S. Gullapalli, and B. Sundén, "CFD Simulation of Heat Transfer and Pressure Drop in Compact Brazed Plate Heat Exchangers," *Heat Transfer Engineering*, 35(4), pp. 358–366, 2013.
[22] C. Büyükaşik, "Computational heat and fluid flow analysis of an innovative plate for a plate heat," *Master Thesis*, Çukurova University, Adana, Turkiye, 2020.
[23] G. Peker, C. Yıldız, G. Çakmak, Y. Bilgiç, and A. Yıldız, "Thermal performance of new type plate heat exchanger with spring turbulence generator using nanofluid flow," *Experimental Heat Transfer*, Early Access, 2022.
[24] H. Mehrarad, M. R. Sarmasti Emami, and K. Afsari, "Thermal performance and flow analysis in a brazed plate heat exchanger using MWCNT@water/EG nanofluid," *International Communications in Heat and Mass Transfer*, vol. 146, pp. 106867, Jul 2023.
[25] S. Gungor, "Experimental comparison on energy consumption and heat transfer performance of corrugated H-type and L-type brazed plate heat exchangers," *International Communications in Heat and Mass Transfer*, vol. 144, pp. 106763, 2023.
[26] J. Berce, M. Zupančič, M. Može, and I. Golobič, "Infrared thermography observations of crystallization fouling in a plate heat exchanger," *Applied Thermal Engineering*, vol. 224, pp. 120116, 2023.

Biographies

Kadir Cebeci received his B.S. degree in Mechanical Engineering from Gaziantep University in 2020. He attended Aydın Adnan Menderes University as a Master's degree student and completed his degree in Mechanical Engineering in 2023. Currently Mr. Cebeci Works in BOSCH Turkiye as an R&D Design Engineer. His work focuses on the design of cost and energy-efficient boiler designs.
E-mail: Kadir.Cebeci@bosch.com.tr

Sinan Güçlüer received his B.S. degree in Mechanical Engineering from Mustafa Kemal University in 2004. Dr. Güçlüer also obtained his M.Sc. degree in Mechanical Engineering from Mustafa Kemal University in 2007. Dr. Güçlüer earned his Ph.D. degree in Mechanical Engineering from Gazi University in 2017. Currently, he is an Assistant Professor of Mechanical Engineering at Aydın Adnan Menderes University, and he works on heat transfer, thermal science, microfluidic systems, MEMS, and lab-on-chip applications.
E-mail: sgucluer@adu.edu.tr